

CMU-HEP93-23  
(DOE-ER/40682-48)

## Isoscalar-isovector mass splittings in excited mesons

Paul Geiger

*Physics Department, Carnegie Mellon University, Pittsburgh, PA 15213*

### Abstract

Mass splittings between the isovector and isoscalar members of meson nonets arise in part from hadronic loop diagrams which violate the Okubo-Zweig-Iizuka rule. Using a model for these loop processes which works qualitatively well in the established nonets, I tabulate predictions for the splittings and associated isoscalar mixing angles in the remaining nonets below about 2.5 GeV, and explain some of their systematic features. The results for excited vector mesons compare favorably with experiment.

12.40.Aa, 12.38.Aw, 13.25.+m. 14.40.Cs

Typeset using REVTEX

The established meson nonets, with the exception of the pseudoscalars, exhibit two notable regularities: (i) the isoscalar members (which we shall generically denote by  $\mathcal{F}$  and  $\mathcal{F}'$ ) are almost ideally mixed:  $\mathcal{F} \approx \frac{u\bar{u}+d\bar{d}}{\sqrt{2}}$  and  $\mathcal{F}' \approx s\bar{s}$ , and (ii) the  $\mathcal{F}$  is nearly degenerate with its isovector partner,  $\mathcal{A}$ . Though the  $U(1)$  anomaly spoils these two rules of thumb in the  $0^{-+}$  sector, they hold well enough in  $1^{--}$ ,  $1^{+-}$ ,  $1^{++}$ ,  $2^{++}$ ,  $3^{--}$  and  $4^{++}$  mesons that one may easily forget they are not underwritten by any firm theoretical considerations. For while we should expect violations of (i) and (ii) to be suppressed because they entail violations of the Okubo-Zweig-Iizuka (OZI) rule [1] (the  $\mathcal{F} - \mathcal{A}$  splitting is proportional to the amplitude  $A$  for  $u\bar{u} \leftrightarrow d\bar{d}$  mixing and the  $\mathcal{F} - \mathcal{F}'$  mixing angle is proportional to the amplitude  $A'$  for  $\{u\bar{u} \text{ or } d\bar{d}\} \leftrightarrow s\bar{s}$  mixing), the observed *degree* of suppression does not follow from any general argument. In particular, in the large- $N_c$  expansion  $A$  and  $A'$  are proportional to  $N_c^{-1}$ , the same as a typical OZI-allowed hadronic width, leading one to expect mass splittings  $M_{\mathcal{F}} - M_{\mathcal{A}}$  of order 100 MeV and mixing angles  $\theta - \theta_{\text{ideal}}$  of order  $\tan^{-1}(1/2)$ .

In fact, Fig. 1 suggests a specific mechanism for generating substantial  $A$  and  $A'$ : even if we suppose that the “pure annihilation” time-ordering of Fig. 1(a) is small, it seems difficult to arrange a suppression of the hadronic loop diagram in Fig. 1(b) since the vertices there are OZI-allowed and the loop momentum runs up to  $\sim \Lambda_{\text{QCD}}$  before it is cut off by the meson wavefunctions. This instance of a “higher-order paradox” [2] was investigated in detail in Refs. [3,4]. There it was found that, while individual intermediate states (such as  $\pi\pi$ ,  $\omega\pi$ , *etc.*) do indeed each contribute  $\sim 100$  MeV to  $A$  and  $A'$ , the sum over *all* such states tends to give a much smaller net result, of order 10 MeV in most nonets. In essence, this occurs because the constituent quark and antiquark created at the lower vertex of Fig. 1(b) emerge in a dominantly  ${}^3P_0$  relative wavefunction (a result inferred from meson decay phenomenology [5,6]) and the sum over intermediate states turns out to closely approximate a closure sum in which the created quarks retain their original quantum numbers, hence they have no overlap with the final state meson in all nonets except  $0^{++}$ .

An obvious corollary to this explanation is that properties (i) and (ii) may break down appreciably for scalar mesons; this scenario was examined in Ref. [4]. However, smaller deviations can also be expected in other nonets, simply because the cancellations among the loop diagrams are not always perfect. In fact, as we will see, the cancellations are *expected* to be less complete for some excited nonets. In this paper I present predictions for the loop-induced  $\mathcal{F} - \mathcal{A}$  splittings and  $\mathcal{F} - \mathcal{F}'$  mixing angles in excited meson nonets, and explain some systematics of these predictions. The excited vector mesons are particularly interesting, as the available experimental data indicates a sizable  $\mathcal{F} - \mathcal{A}$  splitting in both the  $2^3S_1$  and  ${}^3D_1$  sectors.

The mixing amplitude of Fig. 1(b) is given by

$$A(E) = \sum_n \frac{\langle d\bar{d}|H_{pc}^{u\bar{u}}|n\rangle \langle n|H_{pc}^{d\bar{d}}|u\bar{u}\rangle}{(E - E_n)}, \quad (1)$$

where the sum is over a complete set of two-meson intermediate states  $\{|n\rangle\}$ , and  $H_{pc}^{f\bar{f}}$  is a quark pair creation operator for the flavor  $f$ . Similar formulas of course apply for  $A'(E)$  and  $A''(E)$  (the latter denotes the amplitude for  $s\bar{s} \leftrightarrow s\bar{s}$  mixing). The  ${}^3P_0$  decay model

leads to the following expression for the 3-meson vertices:

$$\begin{aligned} \langle A | H_{pc} | BC \rangle &= \frac{2}{(2\pi)^{3/2}} \gamma_0 \phi \boldsymbol{\Sigma} \cdot \int d^3k d^3p d^3p' \Psi(\mathbf{p}, \mathbf{p}') \Phi_B^*(\mathbf{k} + \frac{\mathbf{p}'}{2}) \Phi_C^*(\mathbf{k} - \frac{\mathbf{p}'}{2}) \\ &\times (\mathbf{k} + \frac{\mathbf{q}}{2}) \exp[-\frac{2r_q^2}{3}(\mathbf{k} + \frac{\mathbf{q}}{2})^2] \Phi_A(\mathbf{k} - \frac{\mathbf{q}}{2} - \mathbf{p}). \end{aligned} \quad (2)$$

Here the  $\Phi$ 's are meson wavefunctions (which out of computational necessity we take to be harmonic oscillator wavefunctions), while  $\phi$  and  $\boldsymbol{\Sigma}$  are flavor and spin overlaps, respectively. The matrix element is evaluated in the rest frame of the initial meson  $A$  so that  $\mathbf{P}_B = -\mathbf{P}_C \equiv \mathbf{q}$ . The intrinsic pair creation strength,  $\gamma_0$ , and the “constituent quark radius,”  $r_q$ , are parameters which we fit to measured decay widths. The function  $\Psi(\mathbf{p}, \mathbf{p}')$  contains a flux-overlap factor that arises in the flux-tube breaking model [6], and also a “color-transparency” factor, which incorporates a reduction in the pair creation amplitude when the quark and antiquark in meson  $A$  are close enough to screen each other's color charges [7]. The intermediate states are labeled by the oscillator quantum numbers  $\{n, \ell, m, S, S_z\}$  of mesons B and C, plus the momentum and angular momentum of the relative coordinate. Most of the contribution to  $A(E)$  comes from low-lying states ( $\ell_B, \ell_C \lesssim 3$  and  $n_B, n_C \lesssim 1$ ) but we sum up to  $\ell_B, \ell_C \approx 8$  and  $n_B, n_C \approx 4$  in order to see good convergence.

By writing the mixing amplitudes as contributions to meson mass matrices,

$$M = \begin{bmatrix} m + A & A & A' \\ A & m + A & A' \\ A' & A' & m + \Delta m + A'' \end{bmatrix}, \quad (3)$$

in the  $\{u\bar{u}, d\bar{d}, s\bar{s}\}$  basis, or

$$M = \begin{bmatrix} m & 0 & 0 \\ 0 & m + 2A & \sqrt{2}A' \\ 0 & \sqrt{2}A' & m + \Delta m + A'' \end{bmatrix}. \quad (4)$$

in the  $\{\frac{(u\bar{u}-d\bar{d})}{\sqrt{2}}, \frac{(u\bar{u}+d\bar{d})}{\sqrt{2}}, s\bar{s}\}$  basis, one sees that, when the mixings are small,  $2A$  is the  $\mathcal{F} - \mathcal{A}$  mass difference and  $\sqrt{2}A'/\Delta m$  is the  $\mathcal{F} - \mathcal{F}'$  mixing angle.

Equation (2) and our techniques for computing it, our procedure for fitting its parameters, and our sensitivity to those parameters, are discussed in detail in Refs. [3,4].

Table I contains our results. The  $^3S_1$ ,  $^1P_1$ ,  $^3P_1$ ,  $^3P_2$ ,  $^3D_3$ , and  $^3F_4$  nonets were already analyzed in Ref. [4]; we include them here to illustrate the level of accuracy that may be expected for the new predictions [8]. (Note that the rather poor  $^3P_2$  prediction is by far the most sensitive to parameter changes – it moves from  $-3$  MeV to  $-38$  MeV when  $\beta$  is changed from  $0.40$  GeV to  $0.45$  GeV.) By also taking into account the stability of our results under parameter variations, as well as the observed accuracy of the decay analysis in Ref. [6], we estimate that our mass-splitting predictions are reliable up to a factor of two or so.

While the mass splittings mainly measure  $A$ , mixing angles give information about  $A'$ . The mixing angles in column 3 are defined by

$$\begin{aligned}\mathcal{F} &= \left| \frac{u\bar{u} + d\bar{d}}{\sqrt{2}} \right\rangle \cos \phi - |s\bar{s}\rangle \sin \phi \\ \mathcal{F}' &= \left| \frac{u\bar{u} + d\bar{d}}{\sqrt{2}} \right\rangle \sin \phi + |s\bar{s}\rangle \cos \phi .\end{aligned}\quad (5)$$

Note that  $\phi = \theta - \theta_{\text{ideal}}$ , where  $\theta$  is the octet-singlet mixing angle and  $\theta_{\text{ideal}} = \tan^{-1}(1/\sqrt{2})$ . We do not list experimental results for mixing angles since their extraction from meson masses is very model dependent [9], and though they are measured quite directly by decay branching ratios, these ratios are known only poorly for the interesting (*i.e.*, substantially mixed)  $^1P_1$  and  $^3P_1$  states. As with the mass splittings, our values for  $\theta - \theta_{\text{ideal}}$  should only be trusted to within a factor of about two. Such large theoretical uncertainties of course mean that Table I can only be taken as a rough guide. Nevertheless, it clearly contains some definite qualitative predictions. Most interesting are the excited vectors,  $2^3S_1$  and  $^3D_1$ ; some properties of these states have been extracted from  $e^+e^-$  experiments [9,10], so we can compare with our calculations. For the radial excitations, we find  $m_{\omega'} - m_{\rho'} = -53$  MeV and  $\phi = -26^\circ$ . Most of the splitting here comes from  $A'$  rather than  $A$ , *i.e.*, just as with the  $^3P_1$  nonet, strange intermediate states (in particular  $K^*\bar{K} + \bar{K}^*K$ ) are the source of most of the OZI-violation. The predicted mixing angle is quite large but has only moderate effects on the branching ratios to non-strange final states, since the flavor overlaps for such decays are proportional to  $\cos^2 \phi$ . Thus, for example, we find that  $\frac{\Gamma(\omega' \rightarrow \rho\pi)}{\Gamma(\rho' \rightarrow \omega\pi)}$  is reduced from 3 to 2.4 by the flavor overlap factor (and suffers a further reduction to about 1.9 due to the decreased phase space of the  $\omega'$ ). On the other hand, the flavor-overlap part of  $\frac{\Gamma(\omega' \rightarrow K^*\bar{K})}{\Gamma(\omega' \rightarrow K\bar{K})}$ , which goes like  $\left| \frac{\cos \phi - \sqrt{2} \sin \phi}{\cos \phi + \sqrt{2} \sin \phi} \right|^2$ , is enhanced by a factor of almost 30 over the ideal-mixing prediction. The flux-tube breaking model of Ref. [6] (which is probably reliable to within a factor of 2) predicts  $\Gamma(\omega' \rightarrow K^*\bar{K}) \approx 20$  MeV and  $\Gamma(\omega' \rightarrow K\bar{K}) \approx 30$  MeV for an ideally mixed  $\omega'$ ; with our mixing angle of  $-26^\circ$  the predictions become approximately 40 MeV and 2 MeV, respectively [11].

The mixing amplitudes in the  $^3D_1$  nonet are unusually large:  $A \approx -130$  MeV and  $A' \approx -160$  MeV, thus our perturbative calculation is probably less trustworthy here than in other nonets. Nevertheless we have significant qualitative agreement with the experimental  $\omega'' - \rho''$  splitting of  $(-106 \pm 23)$  MeV – the largest measured splitting in Table I. The biggest individual contributions to  $A$  in this sector come from the  $a_0 \rho''$  and  $a_1 \rho''$  intermediate states. The phenomenology of the large negative  $^3D_1$  mixing angle is very similar to the  $2^3S_1$  case:  $\frac{\Gamma(\omega'' \rightarrow \rho\pi)}{\Gamma(\rho'' \rightarrow \omega\pi)}$  is reduced to about 2, and the predictions of Ref. [6],  $\Gamma(\omega'' \rightarrow K^*\bar{K}) \approx 10$  MeV and  $\Gamma(\omega'' \rightarrow K\bar{K}) \approx 40$  MeV become approximately 20 MeV and 3 MeV, respectively.

A final comment on the results of Table I concerns the average magnitudes of  $M_{\mathcal{F}} - M_A$  and  $\theta - \theta_{\text{ideal}}$  in the various nonets. Confining attention to the radial ground states, the apparent trend is for the mixings to start out small in the S-wave mesons, become considerably larger in the P and D wave nonets and then decrease again for the F and G (and higher) nonets. This pattern can be understood as follows. It was shown in Ref. [3] that for a particular choice of the pair creation form factor, the closure sum corresponding to Eq. (1) can be written as a power series in a variable  $\lambda$  which is a function only of  $\beta$  and  $r_q$ . The coefficient of the  $\lambda^k$  term is the sum of all loop graphs whose intermediate states satisfy  $2(n_b + n_c) + (\ell_b + \ell_c + \ell_{\text{rel}}) = k$ . Since the closure sum vanishes for any  $\lambda$ , it follows that each

subset of graphs corresponding to a particular value of  $2(n_b + n_c) + (\ell_b + \ell_c + \ell_{\text{rel}}) \equiv 2N + L$  sums to zero. (For example, in the  $N = 0$  sector, intermediate states containing two S-wave mesons in a relative P-wave exactly cancel with intermediate states where an S-wave meson and a P-wave meson are in a relative S-wave.) The intermediate mesons in each subset have similar masses, hence the cancellation tends to persist in the full calculation with energy denominators. With P- and D-wave initial states, the terms with  $(2N + L = \text{constant})$  no longer exactly cancel; some of the  $(2N + L = \text{constant} + 2)$  terms must be added [12], and the significant mass splittings among such states tends to spoil the cancellations when energy denominators are inserted. For F- and G-wave initial states the cancellation requires the  $(2N + L = \text{constant})$ ,  $(2N + L = \text{constant} + 2)$ , and  $(2N + L = \text{constant} + 4)$  terms, so one might expect even worse deviations from the closure result. However, some of these terms vanish identically because the highly excited initial state does not couple to them: in the  ${}^3P_0$  model, the orbital angular momentum of the initial state,  $\ell_A$ , can differ from  $L$  by at most one unit, thus (for example) F-wave mesons do not couple at all to intermediate states which have  $L = 0$ . Hyperfine splittings in the  $L = 0$  sector cause the largest deviations from closure (note also that deviations due to radial and orbital splittings are largest among low-lying intermediate states), thus by decoupling from  $L = 0$  the F- and G-wave mesons end up experiencing less OZI-violation than P- and D-wave mesons.

In summary, Table I ought to provide a useful rough guide to isoscalar-isovector mass splittings and mixing angles in excited meson nonets. There is no good reason to expect  $|M_F - M_A| \lesssim 10$  MeV in general. In fact, it is probable that the splittings in P- and D-wave mesons, as well as in radial excitations, will be substantial.

I thank Nathan Isgur for discussions. This research has been supported, in part, by an NSERC of Canada fellowship and by the U.S. Dept. of Energy under grant No. DE-FG02-91ER40682.

## REFERENCES

- [1] S. Okubo, Phys. Lett. **5**, 1975 (1963); Phys. Rev. D **16**, 2336 (1977); G. Zweig, CERN Report No. 8419 TH 412, 1964 (unpublished); reprinted in *Developments in the Quark Theory of Hadrons*, edited by D. B. Lichtenberg and S. P. Rosen (Hadronic Press, Massachusetts, 1980); J. Iizuka, K. Okada, and O. Shito, Prog. Th. Phys. **35**, 1061 (1965); J. Iizuka, Prog. Th. Phys. Suppl. **37**, 38 (1966).
- [2] H.J. Lipkin, Nucl. Phys. B **291**, 720 (1987); Phys. Lett. B **179**, 278 (1986); Nucl. Phys. B **244**, 147 (1984); Phys. Lett. B **124**, 509 (1983).
- [3] P. Geiger and N. Isgur, Phys. Rev. D **44**, 799 (1991); Phys. Rev. Lett. **67**, 1066 (1991).
- [4] P. Geiger and N. Isgur, Phys. Rev. D **47**, 5050 (1993).
- [5] The  $^3P_0$  model was developed by L. Micu, Nucl. Phys. B **10**, 521 (1969); A. Le Yaouanc, L. Oliver, O. Pene, and J.C. Raynal, Phys. Rev. D **8**, 2223 (1973); **9**, 1415 (1974); **11**, 1272 (1975); M. Chaichian and R. Korgerler, Ann. Phys. (N.Y.) **124**, 61 (1980). See also A. Le Yaouanc, L. Oliver, O. Pene, and J.C. Raynal, *Hadron Transitions in the Quark Model* (Gordon and Breach, 1988). The model has been extensively applied to hadronic loop calculations – see N.A. Tornquist, Acta Phys. Polonica B **16**, 503 (1985) and references therein.
- [6] R. Kokoski and N. Isgur, Phys. Rev. D **35**, 907 (1987).
- [7] The parameters used in the present calculation are the same as those used in (the third column Table I of) Ref. [4]:  $r_q = 0.25$  fm,  $\beta = 0.40$  GeV,  $b = 0.18$  GeV $^2$ , and  $t = g = 1$ .
- [8] Note that in [4] we simply reported the  $A$  and  $A'$  amplitudes while in this paper we have inserted them into the mass matrices and diagonalized. In practice this has negligible effects on the numerical results, except in the  $^3P_1$  and  $^2S_1$  nonets, where  $|A'|$  is significantly larger than  $|A|$  so that most of the mass splitting actually comes from  $A'$ .
- [9] Particle Data Group, K. Hikasa *et al.*, Phys. Rev. D**45**, S1 (1992).
- [10] A. Donnachie and A.B. Clegg, Z. Phys. C **51**, 689 (1991); **42**, 663 (1989).
- [11] Note that we have calculated only the real parts of the mixing amplitudes; a significant imaginary component in  $A'$  would alter these branching ratio predictions.
- [12] Note that parity requires  $L$  to be even (odd) whenever  $\ell_A$  is odd (even).

## FIGURES

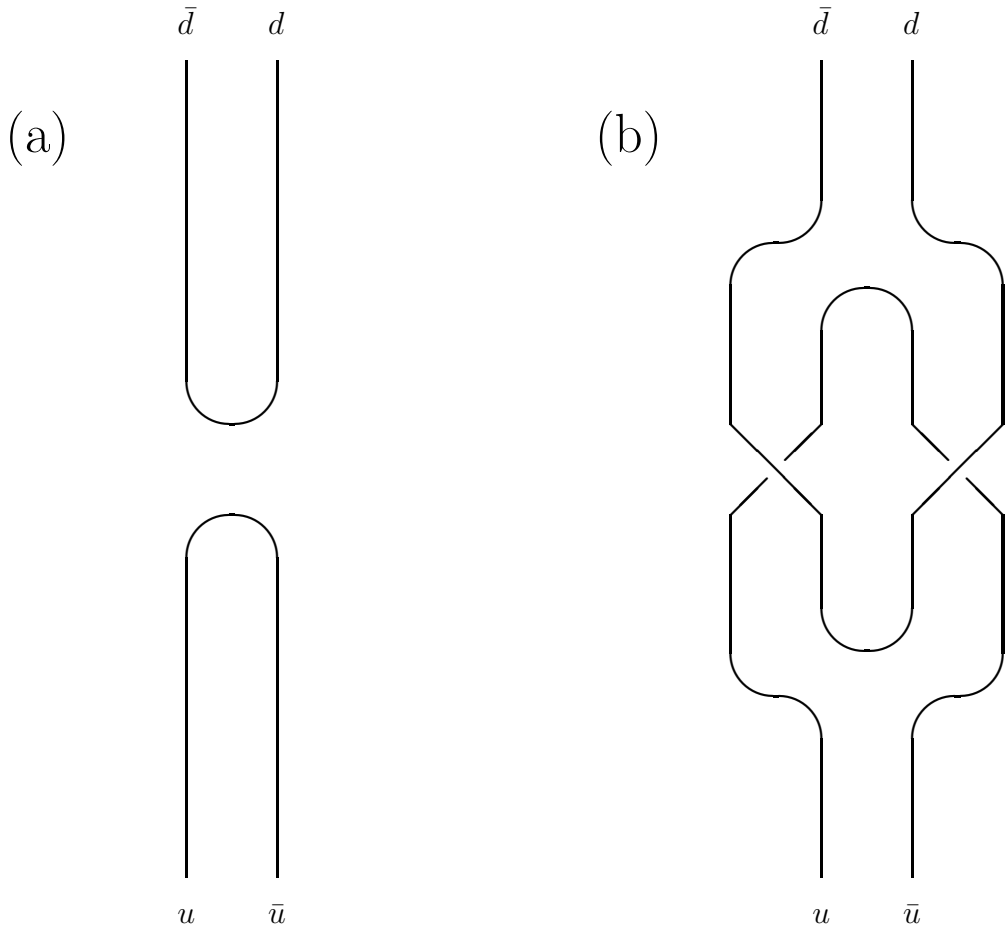


FIG. 1. (a) OZI-violation by “pure annihilation.” (b) A different time ordering of the same Feynman graph gives OZI-violation via two OZI-allowed amplitudes. (In both cases, time flows upward.)

## TABLES

TABLE I. Mass splittings and mixing angles from hadronic loops. The measured values are taken from Ref. [9].

Nonet	Predicted $M_{\mathcal{F}} - M_{\mathcal{A}}$ (MeV)	Measured $M_{\mathcal{F}} - M_{\mathcal{A}}$ (MeV)	Predicted $\theta - \theta_{\text{ideal}}$ (degrees)
$^3S_1$	4	$14 \pm 2$	-1
$2^3S_1$	-53	$-71 \pm 30$	-26
$3^3S_1$	-51		-3
$^1P_1$	-63	$-64 \pm 24$	-15
$^3P_1$	-18	$22 \pm 30$	24
$^3P_2$	-3 to -38 <sup>a</sup>	$-44 \pm 6$	-7
$2^1P_1$	42		11
$2^3P_1$	-48		-7
$2^3P_2$	26		-12
$^1D_2$	-48		-1
$^3D_1$	$\approx -200^{\text{a}}$	$-106 \pm 23$	$\approx -25^{\text{a}}$
$^3D_2$	32		7
$^3D_3$	6	$-24 \pm 8$	1
$2^1D_2$	48		3
$2^3D_1$	-121		-6
$2^3D_2$	-47		-4
$2^3D_3$	-29		-4
$^1F_3$	-2		5
$^3F_2$	-2		0
$^3F_3$	-21		-7
$^3F_4$	28	$12 \pm 36$	-1
$^1G_4$	-1		2
$^3G_3$	-14		1
$^3G_4$	-2		-3
$^3G_5$	-14		-1

<sup>a</sup>See text.